



**HAL**  
open science

## Study of the spatial structure of drift-wave turbulence in the torsatron TJ-K

M. Ramisch, U. Stroth, F. Greiner, N. Mahdizadeh, K. Rahbarnia

► **To cite this version:**

M. Ramisch, U. Stroth, F. Greiner, N. Mahdizadeh, K. Rahbarnia. Study of the spatial structure of drift-wave turbulence in the torsatron TJ-K. 2004. hal-00001832

**HAL Id: hal-00001832**

**<https://hal.science/hal-00001832>**

Preprint submitted on 18 Nov 2004

**HAL** is a multi-disciplinary open access archive for the deposit and dissemination of scientific research documents, whether they are published or not. The documents may come from teaching and research institutions in France or abroad, or from public or private research centers.

L'archive ouverte pluridisciplinaire **HAL**, est destinée au dépôt et à la diffusion de documents scientifiques de niveau recherche, publiés ou non, émanant des établissements d'enseignement et de recherche français ou étrangers, des laboratoires publics ou privés.

# Study of the spatial structure of drift-wave turbulence in the torsatron TJ-K

M. Ramisch<sup>†§</sup>, U. Stroth<sup>‡</sup>, F. Greiner<sup>†</sup>, N. Mahdizadeh<sup>†</sup>,  
K. Rahbarnia<sup>†</sup>

<sup>†</sup> IEAP, University of Kiel, Germany

<sup>‡</sup> IPF, University of Stuttgart, Germany

**Abstract.** The structure and scaling properties of drift-wave turbulence has been studied using a  $8 \times 8$  Langmuir-probe matrix. Quasi-coherent structures drift into the electron-diamagnetic direction. The scalings of correlation lengths and times with the drift scale parameter  $\rho_s$  and other dimensionless parameters are investigated. Using five different gases from hydrogen to argon,  $\rho_s$  could be varied by a factor of 10. A scaling weaker than Bohm-like has been found for the correlation length. The study of  $\rho_s$  scaling on the diffusivity turns out to be misleading since residual dependencies on other parameters are present and the cross-phase between poloidal electric field and density fluctuations is also a function of  $\rho_s$ . The measured turbulent diffusivity is consistent with typical values reported for the edge of fusion plasmas.

## 1. Introduction

Turbulence in the toroidal low-temperature plasma of the torsatron TJ-K [1] is investigated by means of a close comparison between experiment and simulation [2]. In terms of dimensionless parameters, the plasma is similar to that in the edge of fusion devices [3]. Other than in fusion plasmas, however, the low-temperature plasma can be probed by Langmuir probe arrays even in the confinement area with closed field lines.

The objective is a close experiment-theory comparison on a plasma which complies, with respect to turbulence, with the most relevant requirements of a fusion experiment: it is toroidally confined and has centrally peaked pressure profiles. The experimental data are compared with simulations using the drift-Alfvén-wave code DALF3 [4]. A systematic study carried out at the TJ-K plasma parameters in equivalent tokamak geometry showed [3], that the drift-wave dynamic should clearly dominate the interchange drive. The main signature of drift-wave turbulence is a cross-phase between density and potential fluctuations of  $\gamma \approx 0$  on all spatial scales [4, 3]. Experiments using a poloidal probe array

§ Contact: ramisch@physik.uni-kiel.de

to measure cross-phase wavenumber spectra confirmed turbulence in TJ-K to be drift-wave-like [5, 2].

While the structure of drift-wave turbulence parallel to the magnetic field is investigated in another paper of this conference [6], this work presents results on the spatial structure of the fluctuations perpendicular to the field. The experiments have been carried out on discharges with electron-cyclotron-resonance heating (ECRH), whereas results from earlier helicon discharges can be found in Ref. [7]. The paper is organised as follows: The next section introduces the experiment and the  $8 \times 8$  probe matrix, which was the principal diagnostics for this study. The space-time characteristics of quasi-coherent modes are presented in Sec. 3 while Sec. 4 is devoted to scaling studies of the turbulent structures with the relevant dimensionless parameters.

## 2. The torsatron TJ-K, probe matrix and experiments

The torsatron TJ-K has minor and major plasma radii of  $a = 0.1$  m and  $R_0 = 0.6$  m, respectively. It has one helical coil with 6-fold toroidal symmetry producing weak magnetic shear at a rotational transform of  $\iota \approx 1/3$ . Due to ECRH at 2.45 GHz, the magnetic field strength is restricted to the range  $B = 72\text{--}96$  mT on the magnetic axis. Working gases are hydrogen, deuterium, helium, neon and argon at neutral gas pressures of  $2\text{--}5 \times 10^{-5}$  mbar. Typical values for the plasma density are in the range of  $5 \times 10^{17} \text{ m}^{-3}$  and for the electron temperature  $T_e = 5\text{--}10$  eV. The ions are cold ( $T_i \leq 1$  eV).

The 2-dimensional structure of the turbulent fluctuations has been measured using a probe matrix with  $8 \times 8$  tips. As depicted in Fig. 1, each probe consists of a tungsten wire  $200 \mu\text{m}$  in diameter, which is insulated against the plasma by a ceramic tube of  $0.8$  mm diameter. In order to minimise the effective size of the array in poloidal direction, bundles of eight probes, which are stacked in toroidal direction, are mounted on carriers. The vertically (poloidally) oriented probe tips have a length of  $4$  mm. They cover a spatial grid on the low-field side of the poloidal cross-section with a resolution of  $1$  cm in horizontal and vertical direction. The matrix is centred on a variable radial position ranging from  $R - R_0 = 9\text{--}13$  cm in the region of steepest density gradients and highest fluctuation levels. It has been checked, that the matrix does not substantially alter the plasma conditions.

Ion-saturation current fluctuations are simultaneously acquired by means of a 64-channel transient recorder. Each signal consists of  $512$  k values sampled at a frequency of  $f = 1.25$  MHz. For further analyses, the signals are digitally bandpass filtered in a range  $3 \text{ kHz} \leq f \leq 300 \text{ kHz}$ . Experiments have been carried out in five different gases. For each discharge, radial profiles of density, electron temperature and floating potential have been measured by a 1D movable swept Langmuir probe. A transport probe (also movable) is used for simultaneous measurements of local fluctuations in the poloidal electric field and density. This

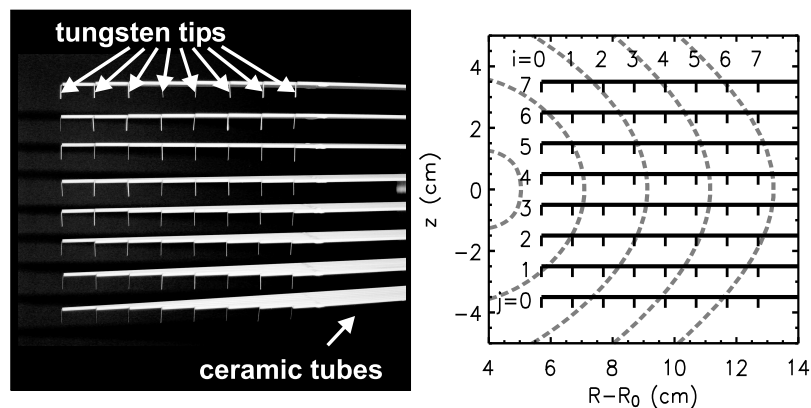


**Figure 1.** Left: view in toroidal direction (parallel to  $B$ ) of the  $8 \times 8$  probe matrix. Probe tips are separated by 1 cm. The white ceramic tubes with a diameter of 0.8 mm and the small tungsten tips bent downward are visible. Right: alignment of the tips in the poloidal cross-section. Calculated flux surfaces up to the separatrix are shown as dashed lines. The horizontal and the vertical probe position will be counted by  $i$  and  $j$ , respectively.

probe consists of three poloidally arranged Langmuir probes [7]. The outer probes measure fluctuations in the floating potential, whereas the centre probe measures fluctuations in the ion-saturation current.

### 3. Space-time structure

Cross-correlation analyses have been carried out on the data obtained by the probe matrix. Figure 2 shows the results for an helium discharge. Fluctuations of the ion saturation current at all tips were correlated to the reference tip  $(i, j) = (3, 3)$ . For different time delays  $\Delta t$  between the probes and the reference, the results were mapped onto the matrix area, revealing the spatio-temporal evolution of quasi-coherent structures in the poloidal cross-section. Radially and poloidally localised structures are observed. They propagate poloidally in the direction of the electron-diamagnetic drift. For  $\Delta t < 0$ , the size of the structure

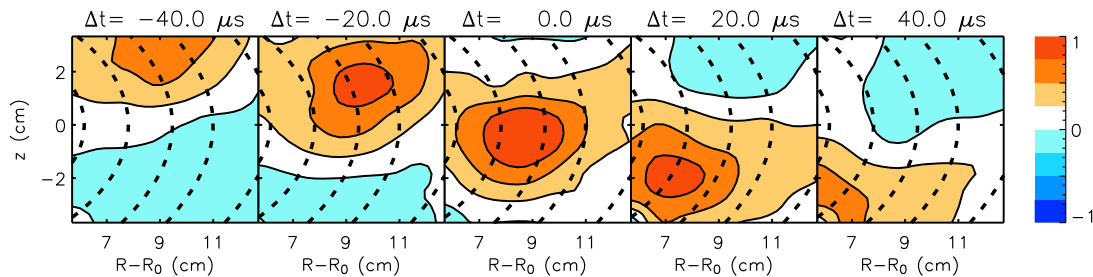


**Figure 2.** Correlation analyses of ion-saturation-current fluctuations within the probe matrix. The reference probe was at  $(i, j) = (3, 3)$ . From left to right the time delay  $\Delta t$  between the probes and the reference was varied from  $-40$ – $40 \mu s$ . Flux surfaces up to the separatrix are depicted as dashed lines.

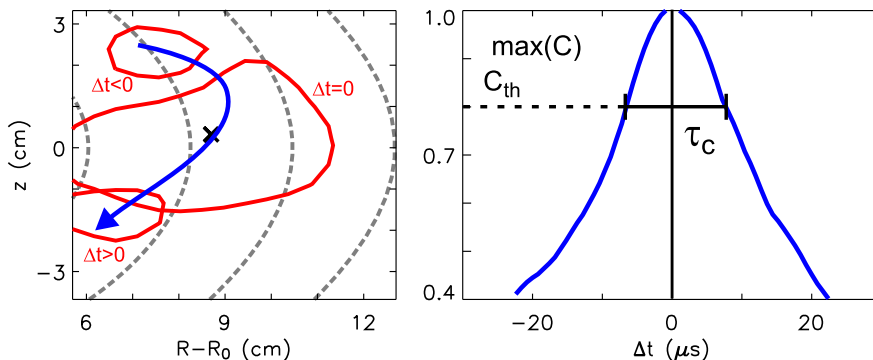


**Figure 3.** Left: contours of the cross-correlation  $C_{i,j} = 0.4$  at three time lags and the trajectory of a density blob as obtained from the contours. The structure grows in time for  $\Delta t < 0$  and decays on its path (arrow) for  $\Delta t > 0$ . A correlation time  $\tau_c$  of the structure is evaluated from the temporal evolution of the maximum correlation by the condition  $\max(C) \geq C_{th}$  (right)

grows, reaches maximum values at  $\Delta t = 0$  and decays again for  $\Delta t > 0$ . The maximum size increases with the ion mass number (see Fig. 7 in Ref. [2]). This dependence will be studied quantitatively below.

#### 4. Scaling properties of the turbulent structures

Theory predicts a linear scaling of the characteristic spatial and temporal scales with the drift-parameter  $\rho_s$  and the inverse of the sound velocity  $a/c_s$ , where

$$\rho_s = \sqrt{T_e M_i / e B} \quad c_s = \sqrt{T_e / M_i}. \quad (1)$$

Here  $M_i$  is the ion mass and  $e$  the elementary charge. In order to investigate this scaling, the correlation length  $L_c$  and the correlation time  $\tau_c$  have been measured in a large number of discharges. For each gas, data have been taken from discharges at two values of the neutral gas pressure ( $2$  and  $5 \times 10^{-5}$  mbar), two of the effective heating powers ( $0.9$  and  $1.8$  kW) and two of the magnetic field strengths ( $72$  and  $89$  mT). Additionally, the matrix was set up on two radial positions, such that turbulent structures could be detected in a radial range of  $R - R_0 = 7 - 14$  cm. Altogether, 220 sets of data have been collected in a data base. For the investigation of the scaling, the radial dependence of all quantities are taken into account. The drift-scale  $\rho_s$  is derived from radial  $T_e$  profiles and the local magnetic field strength  $B$ . Since  $B$  is rather limited due to the resonance condition of ECRH,  $\rho_s$  is mainly varied through the ion mass number of the working gases ranging from 1 to 40.

The relevant quantities have been derived from the correlation analyses as shown in Fig. 3 and described in detail in Ref. [8]. The left part of Fig. 3 reflects the observation of growth and decay – as made in Fig. 2 – for an hydrogen discharge. Here, contours of the cross-correlation for three time lags are shown. The barycentre of the structure has been traced as a function of  $\Delta t$ . The value

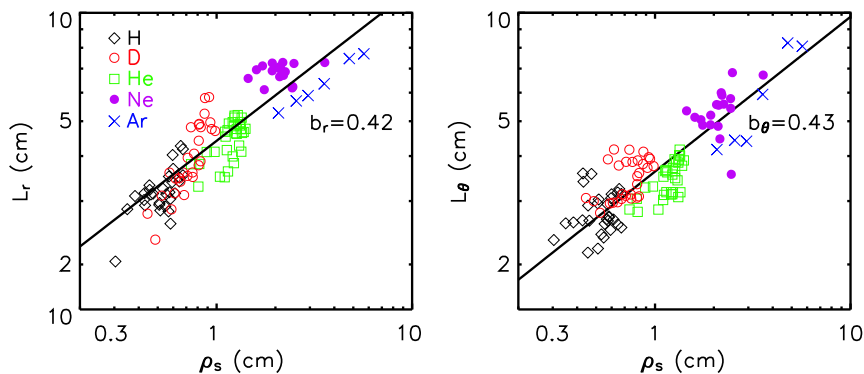


**Figure 4.** Scalings of the radial (left) and poloidal (right) correlation length with  $\rho_s$ .  $L_{r,\theta} \sim \rho_s^{b_{r,\theta}}$  with  $b_r = 0.42$  and  $b_\theta = 0.43$  has been fitted to the data (solid lines).

of maximum correlation is plotted as a function of  $\Delta t$  in the right part of Fig. 3. As indicated in the figure, the duration in which the maximum correlation stays above a value of 0.8 is attributed to the correlation time  $\tau_c$  of the structure. In order to determine the correlation lengths, an ellipse is fitted to a contour line, which is defined by a value of 0.6 for the correlation at  $\Delta t = 0$ .  $L_\theta$  and  $L_r$  are defined by the extensions of the ellipse along the vertical and horizontal lines through the reference point. The values for threshold were set such that for each gas the structure dimensions are covered by the matrix.

For the investigation of the scaling properties of  $L_r$  and  $L_\theta$  with  $\rho_s$ , all data points, for which the drift-ordering constraint does not hold – i.e., all points with  $\rho_s \gtrsim L_n$  – have been omitted. Thus the contribution of argon, which has relatively large drift-scales in comparison to the gradient length, is reduced drastically. In Fig. 4,  $L_r$  and  $L_\theta$  are compared to  $\rho_s$  in a log-log plot. For the radial correlation length a power law according to  $L_r \sim \rho_s^{b_r}$  with  $b_r = 0.42 \pm 0.04$  is obtained from a regression of all gases. The correlation between  $L_r$  and  $\rho_s$  is 82%. For a sub-set including hydrogen and deuterium data only, a stronger dependence with  $b_r^{\text{HD}} = 0.78 \pm 0.14$  at 84% correlation is obtained. The scaling of the poloidal correlation length is comparable to that of  $L_r$  for all gases. A regression yields a scaling with  $b_\theta = 0.43 \pm 0.04$  (at 88% correlation) as shown in Fig. 4, right. This result agrees well with a previous study, where the poloidal correlation length has been evaluated from measurements with a poloidal probe array and a scaling in the range  $L_\theta \sim \rho_s^{1/3-1/2}$  was found [5].

Under the similarity constraint, the parameters  $\beta^*$ ,  $\nu^*$  and  $L_n$  should have been constant for this kind of investigation. For the present data, they actually widely scatter around  $\beta^* \approx 0.1$ ,  $\nu^* \approx 1$  and  $L_n \approx 6$  cm. This spreading is mainly due to neon and argon data. Without these gases, the deviations could be reduced to approximately 60%. A regression analysis, however, did not reveal a significant dependence of the correlation lengths on these parameters.

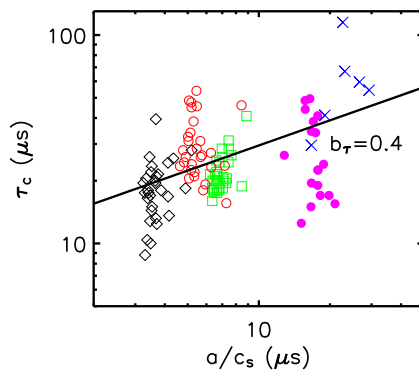


**Figure 5.** Scaling of the correlation time with the inverse sound velocity. A scaling according to  $\tau_c \sim (a/c_s)^{b_\tau}$  is evaluated with  $b_\tau = 0.4$  (solid line).

Fig. 5 depicts the relation of the correlation time  $\tau_c$  to  $a/c_s$ . With the exception of helium, the data exhibit a large scatter for each ion mass. Nevertheless, there is a general trend with the ion mass towards larger correlation times. Due to the large scatter, the correlation between  $\tau_c$  and  $a/c_s$  is in general low ( $<50\%$ ). With  $\tau_c \sim (a/c_s)^{b_\tau}$  a scaling according to  $b_\tau = 0.4 \pm 0.14$  is found. As in the case of  $L_r$ , a stronger dependence with  $b_\tau^{\text{HD}} = 0.8 \pm 0.36$  is obtained for the sub-set including hydrogen and deuterium data only. A significant dependence of  $\tau_c$  on the parameters  $\beta^*$ ,  $\nu^*$  and  $L_n$  has not been observed. More details can be found in Ref. [8]

A simple expression for the turbulent diffusivity is constructed out of the random walk model according to  $D = L_r^2/\tau_c$ . Theory predicts, that for drift-wave turbulence the normalised diffusivity  $D^* = D/D_B$ , where  $D_B = \rho_s c_s$  is the Bohm diffusion coefficient, should scale linear with  $\rho_s$  (gyro-Bohm-like). It turns out, that  $D^*$  scales weaker than gyro-Bohm, as could have been expected from the scalings of  $L_r$  and  $\tau_c$ . For the H-D sub-set, on the other hand, the scaling of the diffusivity does barely reflect the close to linear scalings of  $L_r$  and  $\tau_c$ , pointing to residual dependencies of  $D^*$  on  $a/c_s$  interfering with the scaling. The absolute values of the diffusivity turn out to be rather large with respect to values for the edge of fusion plasmas, which are typically in the range  $0.1\text{--}1\text{ m}^2/\text{s}$  [9, 10]. The values found here for  $D$  are in the range  $20\text{--}200\text{ m}^2/\text{s}$ . In order to compare the absolute values with those of a fusion plasma, the diffusivity has been re-scaled using the ISS95 scaling expression [11] and the relation  $\tau \approx a^2/4D$  under the assumption that the energy confinement time and the particle confinement time scale similarly. The ratio of the ISS95 confinement times between discharges at typical parameters for TJ-K and, e.g., W7-AS is  $\tau^{\text{W7AS}}/\tau^{\text{TJK}} \approx 35$ . Since the minor radius of W7-AS is twice that of TJ-K, the equivalent diffusivity would be still large:  $D^{\text{W7AS}} \approx 0.1 D^{\text{TJK}} \approx 2\text{--}20\text{ m}^2/\text{s}$ .

In this context the cross-phase  $\varphi$  between poloidal electric field fluctuations ( $\tilde{E}_\theta$ ) and density fluctuations ( $\tilde{n}$ ) is examined. For all discharges, the cross-phases are near  $\pi/2$ . This is consistent with a cross-phase  $\gamma$  of zero between density and

potential fluctuations as predicted for drift-wave turbulence and confirmed for TJ-K in Refs. [2, 5]. In the present case, the cross-phases are not constant. They vary from  $\varphi < \pi/2$  for hydrogen, deuterium and helium to  $\varphi > \pi/2$  for argon. Including the cross-phases in the scaling for hydrogen and deuterium alone, a close to gyro-Bohm scaling is found:  $b_D = 0.7 \pm 0.3$ . If the large ion masses are included, the scaling becomes Bohm-like. A more important change occurs to the absolute value of the diffusion coefficient. Including the cross-phase correction reduces the diffusivity by another factor of about 10. Together with the re-scaling to fusion plasma dimensions, the equivalent diffusivity is now in the range 0.2–2 m<sup>2</sup>/s. It could be argued, that a flux-surface-averaged diffusivity would be smaller, since all data have been measured in regions of largest amplitudes on the low-field side. Hence, the value of the diffusivity is in reasonable agreement with values found in the edge of fusion plasmas. Again details can be found in Ref. [8].

## 5. Conclusions

Hydrogen and deuterium discharges, which are practically identical in terms of atomic physics, are consistent with the predicted linear scaling for the turbulent properties  $L_r$  and  $\tau_c$ . Heavier ions tend more to a global Bohm-like scaling. The dimensionless diffusivity based on the simple mixing length expression did not turn out to be an adequate quantity for the investigations of scaling properties. It is rather sensitive to residual dependencies on other parameters than  $\rho_s$  and should be interpreted with caution. More reliable results are obtained, if the basic turbulent properties  $L_r$  and  $\tau_c$  are regarded. The cross-phase between poloidal electric field and density fluctuations substantially modifies the diffusivity and its scaling. Including the cross-phase, the value of the diffusivity is consistent with results from fusion plasmas.

**Acknowledgements:** Financial support by Max-Planck-Institut für Plasmaphysik is gratefully acknowledged. The TJ-K device has been provided by CIEMAT, Madrid.

- [1] Krause N, Lechte C, Stroth U, Niedner S, Ascasibar E and Alonso J, 2002 *Rev. Sci. Instrum.* 73 pp. 3474
- [2] Stroth U, Greiner F, Lechte C, Mahdizadeh N, Rahbarnia K and Ramisch M, 2004 *Phys. Plasmas* 11 pp. 2558
- [3] Niedner S, Scott B D and Stroth U, 2002 *Plasma Phys. Controll. Fusion* 44 pp. 397
- [4] Scott B, 1997 *Plasma Phys. Controll. Fusion* 39 pp. 1635
- [5] Lechte C, Mahdizadeh N, Ramisch M and Stroth U, 2004 *Plasma Phys. Controll. Fusion* Submitted
- [6] Mahdizadeh N, Greiner F, Happel T, Ramisch M and Stroth U *this conference*
- [7] Lechte C, Niedner S and Stroth U, 2002 *New J. Phys.* 4 pp. 34
- [8] Ramisch M, Mahdizadeh N, Stroth U, Greiner F, Lechte C and Rahbarnia K, 2004 *Phys. Plasmas* Submitted
- [9] Gentle K W, Gehre O and Krieger K, 1992 *Nucl. Fusion* 32 pp. 217



- [10] Koponen J P T, Geist T, Stroth U, Dumbrajs O, Hartfuß H *et al.*, 2000 *Nucl. Fusion* 40 pp. 365
- [11] Stroth U, Murakami M, Yamada H, Sano F, Dory R A, Okamura S and Obiki T, 1996 *Nucl. Fusion* 36 pp. 1063